Plasmonics (2020) 15:75–81
https://doi.org/10.1007/s11468-019-01010-y

An Octaband Polarization Insensitive Terahertz Metamaterial Absorber Using Orthogonal Elliptical Ring Resonators

V. K. Verma[1] · S. K. Mishra[2] · K. K. Kaushal[1] · Lekshmi V[1] · Sudhakar S[1] · N. Gupta[3] · B. Appasani[2]

Received: 26 April 2019 / Accepted: 1 August 2019 / Published online: 10 August 2019

Abstract
Terahertz metamaterial absorbers are the latest developments that have tremendous applications in terahertz spectroscopy and terahertz imaging. Especially, the research progressed in the direction of designing multiband absorbers. In this work, a polarization-insensitive metamaterial absorber capable of offering absorption in eight bands is proposed. The unit cell of the absorber consists of two orthogonal elliptical ring resonators (ERRs) that are optimally designed to offer maximum absorption in eight bands. The absorption percentage provided by the structure are 89.46% at 0.63 THz, 99.22% at 1.55 THz, 78.02% at 1.89 THz, 99.27% at 2.33 THz, 99.67% at 2.65 THz, 98.67% at 2.91 THz, 99.64% at 3.22 THz, and 88.02% at 3.42 THz. The absorption characteristics were independent of the polarization angle and thus, the structure is insensitive to variations in polarization angle. This is the first work that reports the design of an octaband terahertz absorber and can find significant use in practical devices.

Keywords Plasma frequency · Terahertz metamaterial absorber · Octaband absorber · Polarization insensitivity

Introduction

In the second half of the twentieth century, many researchers laid the foundations for pioneering the field of electromagnetics. An important contribution in this regard is the paper on negative refractive index by a Russian physicist named V. G. Veselago, who envisions the applications of materials with simultaneous negative permeability and negative permittivity [1, 2]. These materials, now widely known as the metamaterials, have a myriad of applications ranging from microwave to optical frequencies [3–6]. Especially, in the past few years, the research on terahertz metamaterial absorbers (TMA) has gained momentum, owing to the well-known "terahertz gap" and due to their practical utility in spectroscopy and sensing [7, 8].

A TMA consists of a 2-dimensional or 3-dimensional periodic arrangement of unit cells that can absorb the incident electromagnetic radiation. Ideally, these absorbers should be able to absorb the radiation irrespective of its polarization and the angle of incidence. The seminal work on TMA can be attributed to T. J. Yen and his colleagues, who demonstrated the magnetic response at terahertz frequencies using metamaterials [9]. The reduction in the plasma frequency to the anticipated frequency of operation results in the creation of the absorption spectra [10–12]. In the beginning, single-band TMAs were designed but subsequently, researchers attempted to increase the number of absorption bands [13]. Dual-band [14–16], triple-band [17–19], quad-band [20–24], penta-band [25, 26], and hexa-band [27, 28] absorption characteristics were achieved in the terahertz regime. Some of these are complicated as they needed multi-layered structures or concentric ring resonators [21]. So, simple designs that are capable of displaying multiband characteristics are being preferred in the recent years [24–26, 28]. A summary of these important works that are simple to fabricate and having multiband absorption characteristics is given in Table 1.

Thus, from the state of the art, it can be concluded that none of the designed absorbers are capable of displaying more than six absorption bands. For the first time, an octaband TMA is presented in this paper that is made of two orthogonal elliptical ring resonators (ERRs). Moreover, the designed absorber is insensitive for variations in polarization and also displays absorption characteristics for a wide variation in the incidence

✉ B. Appasani
bhargav.appasanifet@kiit.ac.in

[1] Control and Digital Electronics Group, U R Rao Satellite Centre, ISRO, Bengaluru 560017, India

[2] Kalinga Institute of Industrial Technology, Bhubaneswar 751024, India

[3] Birla Institute of Technology, Ranchi 835215, India

Table 1 Multiband TMAs proposed in the literature

Reference	Number of bands	Absorption frequencies (peak absorptivity)	Polarization sensitive	Angle sensitive
[24]	4	1.054 THz (90.6%) 2.16 THz (97.2%) 3.59 THz (93.95%) 3.87 THz (99.61%)	Polarization sensitive in three bands.	Angle insensitive.
[25]	5	1.45 THz (97.78%) 1.80 THz (97.92%) 2.70 THz (96.81%) 3.1 THz (61.07%) 3.7 THz (47.64%)	Polarization insensitive.	Angle insensitive.
[26]	5	0.92 THz (> 98%) 1.58 THz (> 98%) 2.20 THz (> 98%) 2.67 THz (> 98%) 3.33 THz (> 98%)	No analysis has been carried out.	No analysis has been carried out.
[27]	6	0.72 THz (90.6%) 1.62 THz (98.9%) 2.28 THz (99.8%) 2.98 THz (99.5%) 3.41 THz (99.6%) 4.27 THz (95.5%)	No analysis has been carried.	No analysis has been carried.
Proposed	8	0.63 THz (89.46%) 1.55 THz (99.22%) 1.89 THz (78.02%) 2.33 THz (99.27%) 2.65 THz (99.67%) 2.91 THz (98.67%) 3.22 THz (99.64%) 3.42 THz (88.02%)	Polarization insensitive in all the bands.	Both angle sensitive as well as angle insensitive.

angle. In this paper, we present a novel multiband MMA which consists of a single metallic square ring with gaps at the center of three of its sides. The peak absorptivities offered by this structure at various frequencies are 89.46% at 0.63 THz, 99.22% at 1.55 THz, 78.02% at 1.89 THz, 99.27% at 2.33 THz, 99.67% at 2.65 THz, 98.67% at 2.91 THz, 99.64% at 3.22 THz, and 88.02% at 3.42 THz, which are almost the same for all polarization angles. Moreover, four of these eight bands have peak absorptivity of more than 99%, making its design an important contribution for THz imaging application. Another unique feature of the design is that it offers both angle-insensitive and angle-sensitive absorption characteristics depending on the frequency of operation, when the angle of incidence of the electromagnetic wave is varied.

The next section of this paper describes the structural layout of the absorber's unit cell. The various types of simulations carried out on this structure are described in the second section. The choice of the structure's physical dimensions is justified through suitable parametric analysis and the causes of absorption are identified. Finally, important conclusions regarding the work are discussed in the final section of this work.

Structure of the Unit Cell

The structure of the unit cell for the proposed octaband structure is given in Fig. 1. The structure consists of two orthogonal ERRs made up of gold that are fused together and have a thickness of 0.4 μm. The bottom layer is entirely made of gold and has a thickness of 2 μm. This thickness is more than the skin depth, thus making the transmission (T) zero. The dielectric present in between these two layers is made up of gallium arsenide (GaAs) and has a thickness of $h = 8$ μm and has a dielectric constant of $12.94(1+i0.006)$. The other dimensions of the structure are $u = 85$ μm, $a = 70$ μm, $g = 15$ μm, and $b = 40$ μm. These dimensions are optimally set to achieve the multiband absorption characteristics. The absorption factor A becomes unity and the absorber acts as a perfect absorber

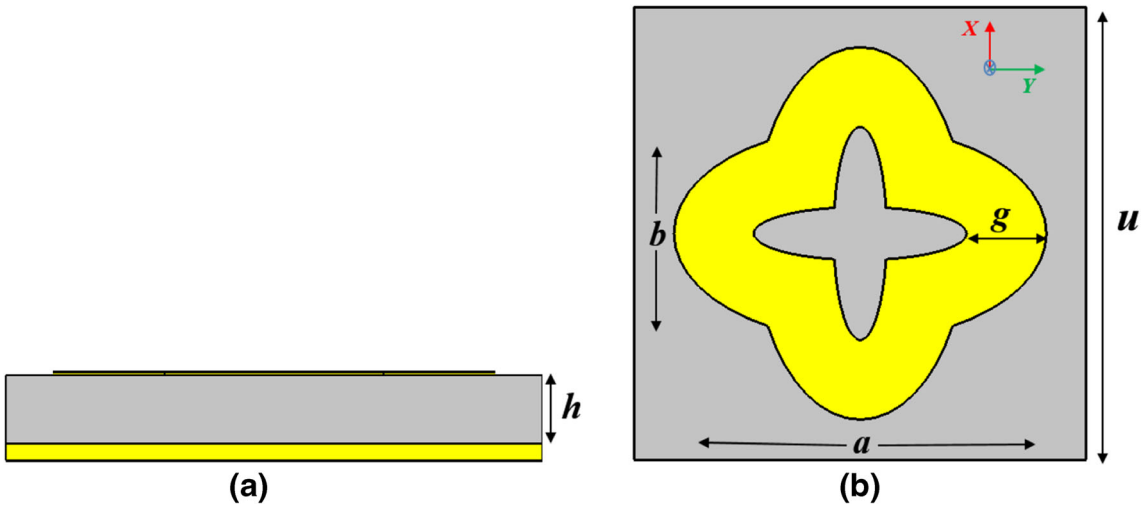

Fig. 1 Unit cell structure. **a** Side view. **b** Top view

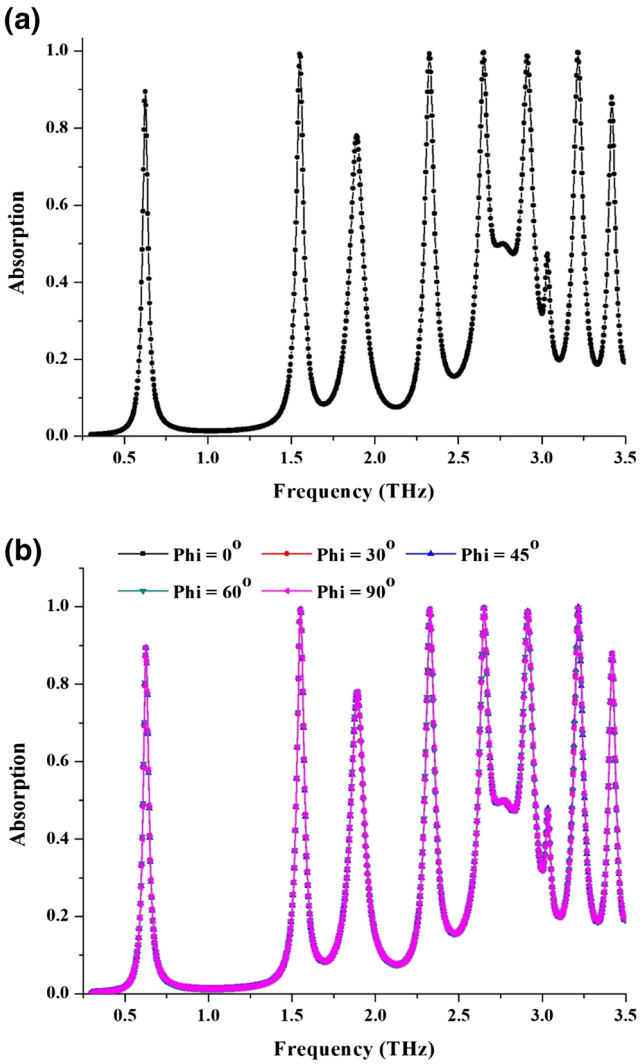

Fig. 2 Absorption characteristics of the proposed absorber for **a** TE polarizations and **b** different polarization angles

when the reflectance becomes zero. The absorber was designed and simulated using the commercially available CST Microwave Studio.

Simulation Results

The octaband absorber provides absorption in eight different bands. Due to its symmetrical design, the absorption characteristics are independent of the variation in polarization angle. The absorption characteristics for TE polarization are shown in Fig. 2a and those for other polarization angles are shown in Fig. 2b.

The absorption bands can be observed between 0.5 and 3.5 THz at eight different frequencies. The peak absorptivityiess in these eight bands are 89.46% at 0.63 THz, 99.22% at 1.55 THz, 78.02% at 1.89 THz, 99.27% at 2.33 THz, 99.67% at 2.65 THz, 98.67% at 2.91 THz, 99.64% at 3.22 THz, and 88.02% at 3.42 THz. Each absorption spectrum also has a bandwidth, which is the range of frequencies over which the absorption is greater than 90%. For absorption spectra having peak absorptivity lower than 90%, other percentages are used for calculating the bandwidth. For example, the first absorption

Table 2 Absorption characteristics of the proposed absorber

Frequency (THz)	Peak absorption	Bandwidth (GHz)
0.63	89.64%	7.4 GHz (> 85% absorption)
1.55	99.22%	18.5 GHz (> 90% absorption)
1.89	78.02%	18.5 GHz (> 75% absorption)
2.33	99.27%	22.2 GHz (> 90% absorption)
2.65	99.67%	22.2 GHz (> 90% absorption)
2.91	98.67%	25.9 GHz (> 90% absorption)
3.22	99.64%	22.2 GHz (> 90% absorption)
3.42	88.02%	7.4 GHz (> 85% absorption)

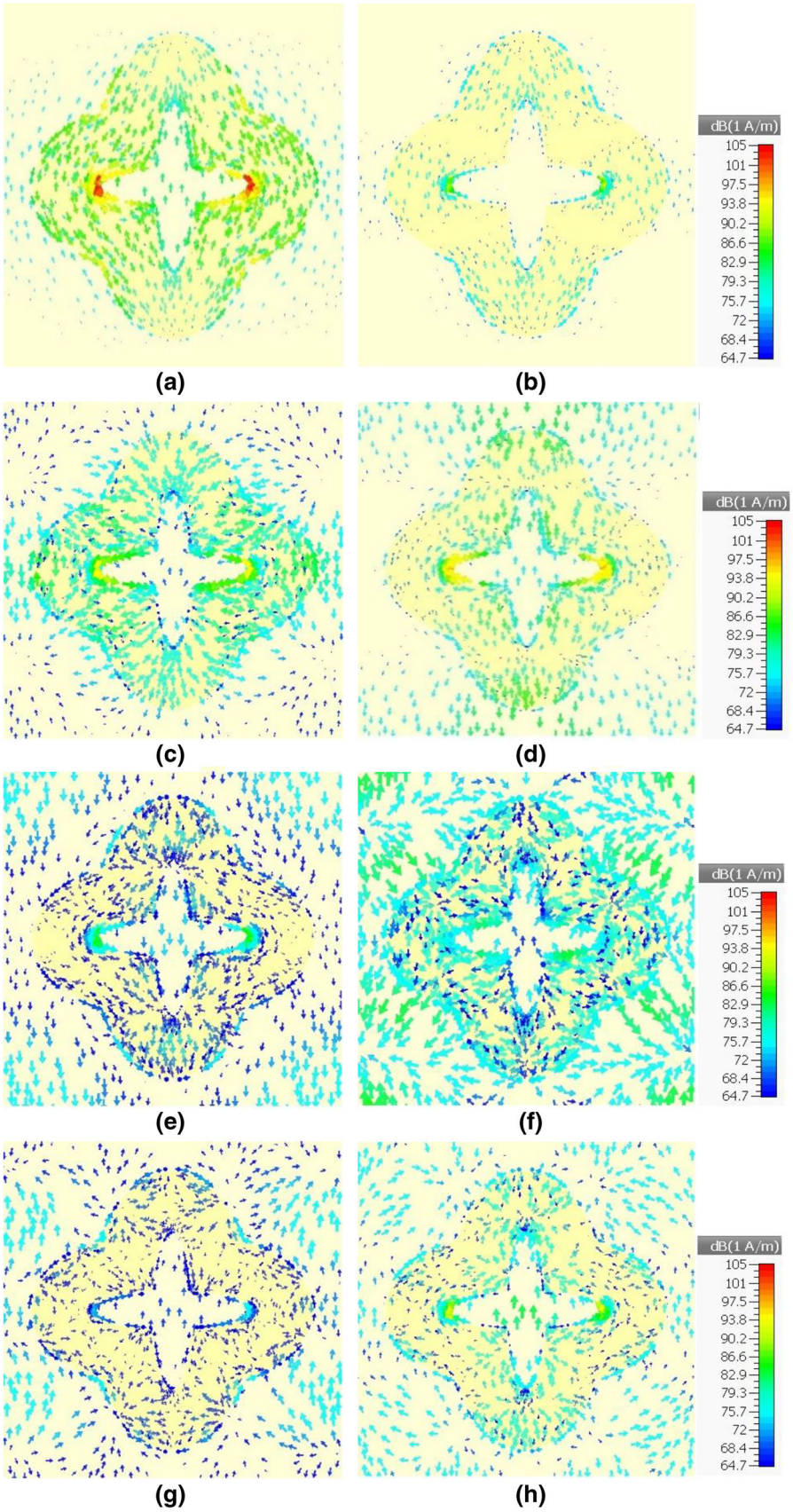

Fig. 3 Current distribution at **a** 0.63 THz, **b** 1.55 THz, **c** 1.89 THz, **d** 2.33 THz, **e** 2.65 THz, **f** 2.91 THz, **g** 3.22 THz, and **h** 3.42 THz

spectrum has a peak absorptivity of 89.64% and its bandwidth is calculated with respect to the 85% absorption criteria. The absorption characteristics in these eight bands are shown in Table 2.

It can be observed from Table 2 that five of the eight absorption bands offer a peak absorption greater than 98%. Two more absorption bands have peak absorption greater than 85%, while the absorption band at 1.89 THz has peak absorption greater than 75%. The mechanism behind the absorption can be further explained with the help of the current distribution diagrams. The current distribution diagram for these eight absorption bands is shown in Fig. 3.

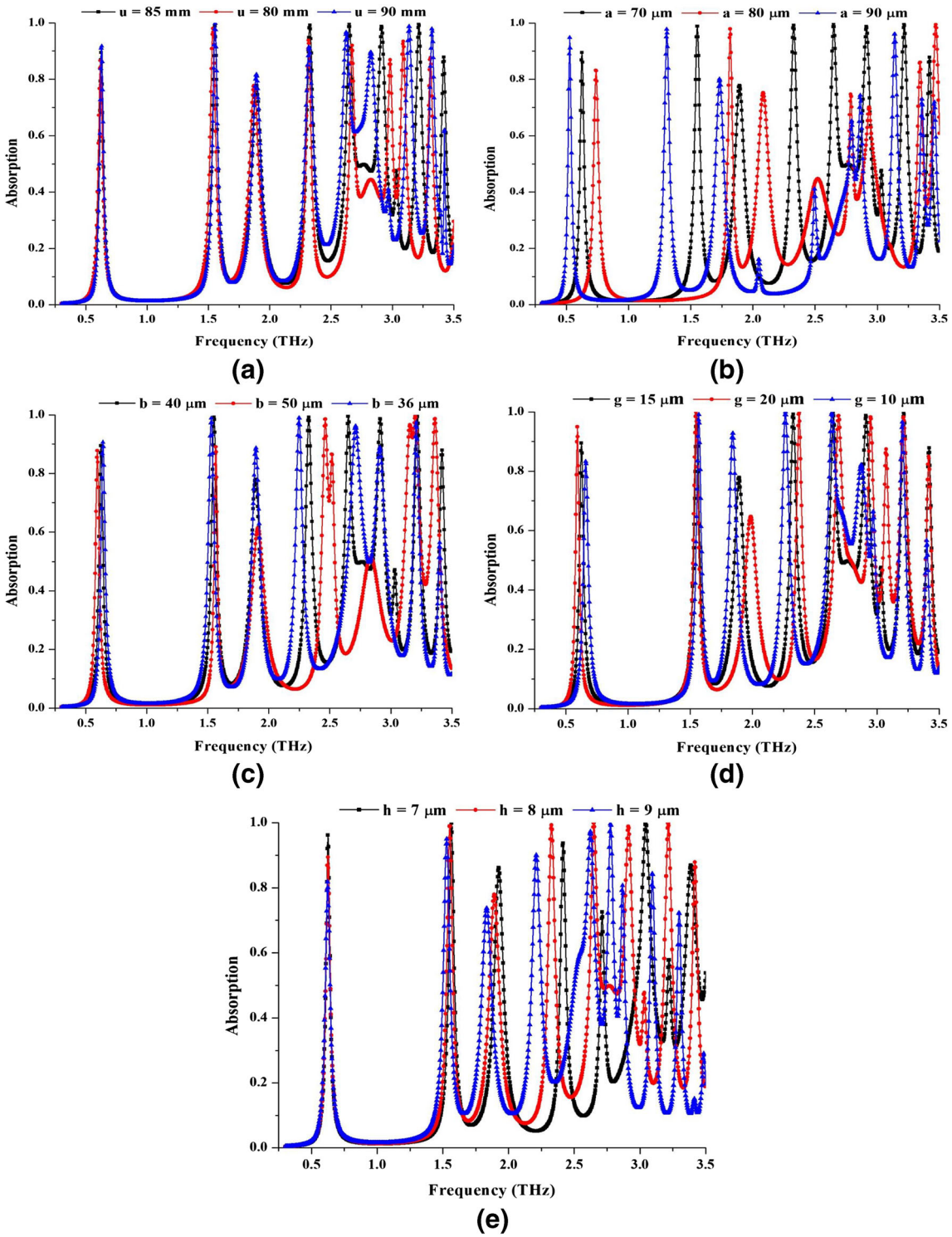

Fig. 4 Variation in the absorption bands for the TE polarization with respect to **a** *u*, **b** *a*, **c** *b*, **d** *g*, and **e** *h*

It can be observed from Fig. 3a that the first absorption mode at 0.63 THz is caused due to the current distribution near the curvature portion of the ERR. Another observation is that the current distribution is maximum at the bends of the ERR, which is due to the slowing of charges near the bends. On the surface of the dielectric, the current is distributed near the edges of the ERR and its direction is opposite to that of the current distribution inside the ERR. At the next higher absorption band observed at 1.55 THz, the current distribution reverses at the middle of the structure indicating a higher order mode. The current distribution in the dielectric is very less and is only present at the metal-dielectric boundary. The third absorption band is observed at 1.89 THz, which is almost thrice the frequency of the first mode. This is also commensurated by the current distribution which changes its direction thrice at the edges of the ERRs. However, the current distribution inside the ERR is normal to the current distribution along the edges. An intermediate fourth absorption peak is observed at 2.33 THz. This mode is an intermediate mode that occurs between the third absorption mode and the fourth absorption mode. The current distribution along the edges of the ERR indicates three changes in the direction of current distribution which is different from that of the current distribution observed at 1.89 THz. Even the current distribution on the surface of the dielectric is different from other modes. Current is distributed only near the top and bottom portions of the unit cell and there is no current distribution at the middle portion of the unit cell. The fifth absorption mode is observed at 2.65 THz and the current distribution changes its direction four times in the ERRs. The changes in the direction of flow of the current can be clearly observed near the edges of the ERR. The current distribution on the surface of the dielectric bends around the edges of the ERR and is unidirectional. For the sixth absorption mode observed at 2.91 THz, the current distribution is denser and stronger than the distribution at 1.89 THz. The seventh absorption mode is observed at 3.22 THz and the current distribution along the edges of the ERR changes its direction six times and the distribution on the surface of the dielectric at the edges of the unit cell changes its direction four times. Finally, the last mode of absorption occurs at 3.42 THz. The current distribution inside the dielectric is similar to the magnetic field of two-pole magnet.

A parametric investigation is carried out, where the design variables are adjusted to analyze their impact on the absorption spectra. The parameters that are analyzed are the unit cell dimension (u), the length of the major axis (a), length of minor axis (b), the width of the resonators (g), and the height of the substrate (h). These results are shown in Fig. 4.

The unit cell dimension (u) when reduced shifts the absorption spectra to higher frequencies but the peak absorptivities get reduced. Increasing this parameter shifts the spectra to lower frequencies but the peak absorptivities get reduced. Thus, the proposed dimension is optimal and either increasing or decreasing this parameter adversely effects the absorption characteristics. Modifying the other parameters, either by increasing or by decreasing their values, results in diminished absorption spectra. Thus, the parametric analysis justifies the choice of the design metrics.

Another important characteristic of an absorber is its ability to absorb electromagnetic spectrum incident on its surface over wide angle of incidence. The effect of incidence angle on the absorption spectra is analyzed and the results are shown in Fig. 5. It can be observed that the absorption spectra at 0.63 THz and at 1.55 THz remain almost unchanged with

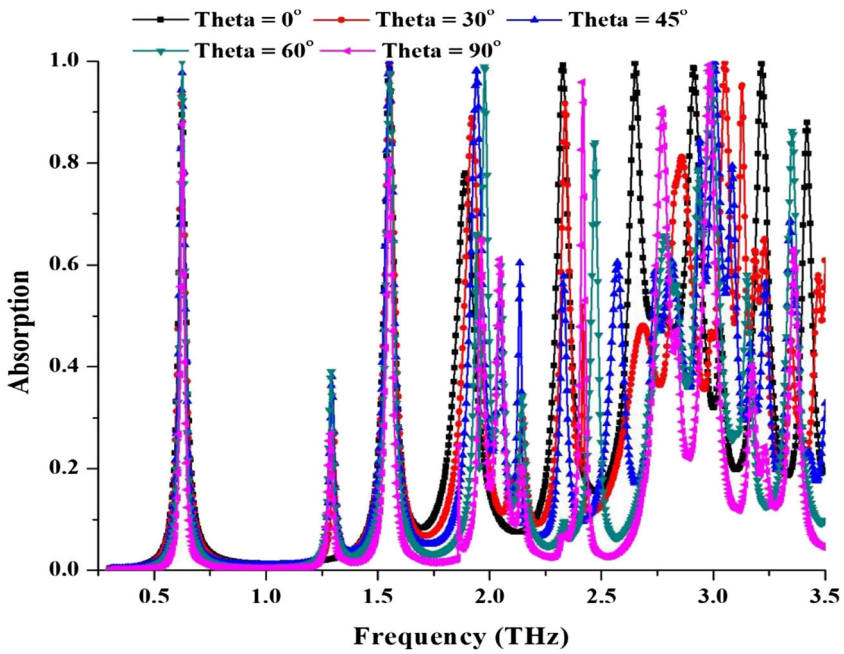

Fig. 5 Absorption characteristics of the proposed absorber for variation in incidence angle

the variation in the angle of incidence. Especially, the 1.55 THz absorption band is extremely significant because of its high absorption (almost 99.22% at normal incidence) and has tremendous applications due to the absorber's insensitivity to variations in polarization and variation in incidence angle at this frequency. The absorption spectra at 1.89 THz is found to slightly shift towards higher frequencies with the increase in incidence angle, but there is also an increase in the amount of absorption offered by the structure. The fourth absorption spectra at 2.33 THz offered angle-insensitive absorption characteristics up to 30° increase in the angle of incidence, but beyond that, the absorption spectra got shifted in frequency and their peak absorptions got diminished. The absorption band at 2.91 THz was almost unchanged except for a slight shift towards higher frequencies with the increase in incidence angle. Thus, the structure offers a combination of both angle-insensitive and angle-sensitive absorption spectra based on the frequency of operation.

Conclusion

Multiband absorbers for terahertz frequency spectrum have practical applications in imaging and spectroscopy. In the recent years, researchers were able to design absorbers that can provide absorption in six bands. This paper proposes an octaband absorber, a first of its kind that is constructed using two orthogonal ERRs. Its polarization insensitivity and angle-sensitive as well as angle-insensitive characteristics are an added advantage to its eight-band absorption spectra. Five of these eight bands have peak absorption greater than 98%. The absorption mechanism has been described using the current distribution diagram and also the parametric analysis has been carried out to justify the design parameters.

References

1. Veselago VG (1968) The electrodynamics of substances with simultaneously negative values of ε and μ. Sov Phys Uspekhi 10(4):509–514
2. Shamonina E, Solymar L (2007) Metamaterials: how the subject started. Metamaterials 1:12–18
3. Smith DR, Padilla WJ, Vier DC, Nemat-Nasser SC, Schultz S (2000) Composite medium with simultaneously negative permeability and permittivity. Phys Rev Lett 84(18):4184–4187
4. Landy NI, Sajuyigbe S, Mock JJ, Smith DR, Padilla WJ (2008) "Perfect metamaterial absorber", Phys Rev Lett, 100
5. Ramakrishna SA, Grzegorczyk TM (2008) Physics and application of negative refractive index materials. CRC Press, Boca Raton
6. Tonouchi M (2007) Cutting-edge terahertz technology. Nat Photonics 1(2):97–105
7. El-Aasser MA (2014) Design optimization of nanostrip metamaterial perfect absorbers. J Nanophotonics 8(1):83–85
8. Siegel PH (2002) Terahertz technology. Microw Theory Tech IEEE Trans 50(3):910–928
9. Yen TJ et al (2004) Terahertz magnetic response from artificial materials. Science 303:1494–1496
10. Rhee JY, Yoo YJ, Kim KW, Kim YJ, Lee YP (2014) Metamaterial-based perfect absorbers. Journal of Electromagnetic Waves and Applications 28(13):1541–1580
11. El-Aasser MA, Mahmoud SA (2019) Spectral properties of plasmonic vertical nano-gap array resonators. J Nanoelectron Optoelectron 14(3):420–424
12. El-Aasser MA, Mahmoud SA (2017) Spectral response of Fabry-Pérot plasmonic optical resonators. Optoelectron Adv Mater Rapid Commun 11:398–404
13. Tao H, Landy NI, Bingham CM, Zhang X, Averitt RD, Padilla WJ (2008) A metamaterial absorber for the terahertz regime: design fabrication and characterization. Opt Express 16:7181–7188
14. Tao H, Bingham CM, Pilon D, Fan K, Strikwerda AC, Shrekenhamer D, Padilla WJ, Zhang X, Averitt RD (2010) A dual band terahertz metamaterial absorber. J Phys D 43:225102
15. Wang BX, Wang GZ, Wang LL (2016) Design of a novel dual-band terahertz metamaterial absorber. Plasmonics 11(2):523–530
16. Shan Y, Chen L, Shi C, Cheng Z, Zang X, Xu B, Zhu Y (2015) Ultrathin flexible dual band terahertz absorber. Opt Commun 350: 63–70
17. Shen X, Cui TJ, Zhao J, Ma HF, Jiang WX, Li H (2011) Polarization-independent wide-angle triple-band metamaterial absorber. Opt Express 19:9401–9407
18. Wang BX, Wang GZ, Sang T (2016) Simple design of novel triple band terahertz metamaterial absorber for sensing application. J Phys D Appl Phys 49:165307–165313
19. Shen X, Yang Y, Zang Y, Gu J, Han J, Zhang W, Jun Cui T (2012) Triple-band terahertz metamaterial absorber: design, experiment, and physical interpretation. Appl Phys Lett 101:154102
20. Liu S, Zhuge J, Ma S, Chen H, Bao D, He Q, Zhou L, Cui TJ (2015) A bi-layered quad-band metamaterial absorber at terahertz frequencies. J Appl Phys 118:245304
21. Wang BX (2017) Quad-band terahertz metamaterial absorber based on the combining of the dipole and quadrupole resonances of two SRRs. IEEE J Sel Top Quantum Electron 23(4):1–7
22. Meng HY, Wang LL, Zhai X, Liu GD, Xia SX (2018) A simple design of a bulti-band terahertz metamaterial absorber based on periodic square metallic layer with T-shaped gap. Plasmonics 13(1):269–274
23. Wang BX, Wang GZ (2016) Quad-band terahertz absorber based on a simple design of metamaterial resonator. IEEE Photonics J 8(6):1–8
24. Appasani B et al. (2018) "A simple multi-band metamaterial absorber with combined polarization sensitive and polarization insensitive characteristics for terahertz applications," Plasmonics, pp. 1–6
25. Mohanty A, Acharya OP, Appasani B, Mohapatra SK (2018) A multi-band terahertz metamaterial absorber based on a II and U-shaped structure. Photonics Nanostruct 32:74–80
26. Wang GZ, Wang BX (2015) Five-band terahertz metamaterial absorber based on a four-gap comb resonator. J Lightwave Technol 33(24):5151–5156
27. Wang BX, Wang GZ, Sang T, Wang LL (2017) Six-band terahertz metamaterial absorber based on the combination of multiple-order responses of metallic patches in a dual-layer stacked resonance structure. Sci Rep 7:41373
28. Hu D, Wang HY, Zhu Q f (2016) Design of six-band terahertz perfect absorber using a simple U-shaped closed-ring resonator. IEEE Photonics J 8(2):1–8